ISSN 1674-1056
http://cpb.iphy.ac.cn
http://iopscience.iop.org/cpb
中国物理 B
Chinese Physics
中国物理 Chinese Physics B

Measurements of argon metastable density using the tunable diode laser absorption spectroscopy in Ar and Ar/O_2

Dao-Man Han(韩道满), Yong-Xin Liu(刘永新), Fei Gao(高飞), Wen-Yao Liu(刘文耀), Jun Xu(徐军), You-Nian Wang(王友年)
Citation: Chin. Phys. B . 2018, 27(6): 065202. **doi:** 10.1088/1674-1056/27/6/065202

Journal homepage: http://cpb.iphy.ac.cn; http://iopscience.iop.org/cpb

What follows is a list of articles you may be interested in

Effect of driving frequency on electron heating in capacitively coupled RF argon glow discharges at low pressure

Tagra Samir, Yue Liu(刘悦), Lu-Lu Zhao(赵璐璐), Yan-Wen Zhou(周艳文)
Chin. Phys. B . 2017, 26(11): 115201. **doi:** 10.1088/1674-1056/26/11/115201

One-dimensional hybrid simulation of the electrical asymmetry effectcaused by the fourth-order harmonic in dual-frequencycapacitively coupled plasma

Shuai Wang(王帅), Hai-Feng Long(龙海凤), Zhen-Hua Bi(毕振华), Wei Jiang(姜巍), Xiang Xu(徐翔), You-Nian Wang(王友年)
Chin. Phys. B . 2016, 25(11): 115202. **doi:** 10.1088/1674-1056/25/11/115202

Modeling of the nanoparticle coagulation in pulsed radio-frequency capacitively coupled C_2H_2discharges

Liu Xiang-Mei, Li Qi-Nan, Li Rui
Chin. Phys. B . 2015, 24(7): 075204. **doi:** 10.1088/1674-1056/24/7/075204

Characteristics of dual-frequency capacitively coupled SF_6/O_2 plasma and plasma texturing of multi-crystalline silicon

Xu Dong-Sheng, Zou Shuai, Xin Yu, Su Xiao-Dong, Wang Xu-Sheng
Chin. Phys. B . 2014, 23(6): 065201. **doi:** 10.1088/1674-1056/23/6/065201

The effects of process conditions on the plasma characteristic in radio-frequency capacitively coupled $SiH_4/NH_3/N_2$ plasmas: Two-dimensional simulations

Liu Xiang-Mei, Song Yuan-Hong, Jiang Wei, Yi Lin
Chin. Phys. B . 2013, 22(4): 045204. **doi:** 10.1088/1674-1056/22/4/045204

Measurements of argon metastable density using the tunable diode laser absorption spectroscopy in Ar and Ar/O_2*

Dao-Man Han(韩道满)[1], Yong-Xin Liu(刘永新)[1,2,†], Fei Gao(高飞)[1], Wen-Yao Liu(刘文耀)[3], Jun Xu(徐军)[1], and You-Nian Wang(王友年)[1]

[1] *Key Laboratory of Materials Modification by Laser, Ion, and Electron Beams (Ministry of Education), School of Physics, Dalian University of Technology, Dalian* 116024, *China*

[2] *National Demonstration Center for Experimental Physics Education, Dalian University of Technology, Dalian* 116024, *China*

[3] *North University of China, Taiyuan* 030051, *China*

(Received 3 February 2018; revised manuscript received 19 March 2018; published online 10 May 2018)

Densities of Ar metastable states $1s_5$ and $1s_3$ are measured by using the tunable diode laser absorption spectroscopy (TDLAS) in Ar and Ar/O_2 mixture dual-frequency capacitively coupled plasma (DF-CCP). We investigate the effects of high-frequency (HF, 60 MHz) power, low-frequency (LF, 2 MHz) power, and working pressure on the density of Ar metastable states for three different gas components (0%, 5%, and 10% oxygen mixed in argon). The dependence of Ar metastable state density on the oxygen content is also studied at different working pressures. It is found that densities of Ar metastable states in discharges with different gas components exhibit different behaviors as HF power increases. With the increase of HF power, the metastable density increases rapidly at the initial stage, and then tends to be saturated at a higher HF power. With a small fraction (5% or 10%) of oxygen added in argon plasma, a similar change of the Ar metastable density with HF power can be observed, but the metastable density is saturated at a higher HF power than in the pure argon discharge. In the DF-CCP, the metastable density is found to be higher than in a single frequency discharge, and has weak dependence on LF power. As working pressure increases, the metastable state density first increases and then decreases, and the pressure value, at which the density maximum occurs, decreases with oxygen content increasing. Besides, adding a small fraction of oxygen into argon plasma will significantly dwindle the metastable state density as a result of quenching loss by oxygen molecules.

Keywords: argon metastable states, tunable diode laser absorption spectroscopy, capacitively coupled plasmas

PACS: 52.70.–m, 52.70.Kz, 52.80.Vp **DOI:** 10.1088/1674-1056/27/6/065202

1. Introduction

Radio-frequency (RF) capacitively coupled plasma (CCP) has been widely studied by many researchers for its extensive applications in semiconductor manufacturing, flat panel displays, and solar cell industries.[1,2] Argon plays an important role in the industrial process when mixed with other reactive gases, and one important reason is that the existence of argon metastable atoms can lead to the dissociation of other gas molecules increasing, thus significantly affecting the plasma properties.[3,4] Argon $1s_5$ and $1s_3$ states are the two main metastable states in argon-containing plasmas, and they have many favorable physicochemical properties. For example, the energy level of the argon metastable atom is above 10 eV with respect to the ground-state atom, and its lifetime is relatively long, which may reach one second.[5] On account of the forbidden spontaneous transition to lower levels, the metastable atom generally has a relatively high density. Moreover, it has a higher collision cross section with electrons, which exceeds that of the ground-state atom by three or four orders of magnitude. Apparently, these properties of argon metastable atoms will definitely affect the discharge process.[6,7] Thus the study of the dependence of the argon metastable atom density on various external parameters and the underlying physics behind it are of great importance.

In recent years, some progress has been made in theoretical and experimental studies about the production and loss process of argon metastable atoms in CCP.[3,4,8–12] In 1994, Sansonnens *et al.*[3] investigated the important role of argon metastable atoms in argon-diluted silane plasma by combining absorption spectroscopy (AS) and time-resolved optical emission spectroscopy (OES). The results showed that the density of metastable atom is substantially reduced with the addition of a small fraction of silane due to molecular quenching, which also greatly increases the silane dissociation rate. McMillin *et al.*[8,9] used planar laser-induced fluorescence (LIF) to measure the two-dimensional distributions of argon metastable density in different gas mixtures. They found that adding some Cl_2 or CF_4 could significantly reduce the metastable density, and cause the metastable spatial profiles to change. This was confirmed by the later simulation results obtained by Rauf *et al.*[10] through using a hybrid plasma equipment model. With

*Project supported by the National Natural Science Foundation of China (Grant Nos. 11335004, 11722541, 11675039, and 11747153) and the Important National Science and Technology Specific Project, China (Grant No. 2011ZX02403-001).

†Corresponding author. E-mail: yxliu129@dlut.edu.cn

© 2018 Chinese Physical Society and IOP Publishing Ltd

a self-consistent fluid model, Zhang *et al.*[4] investigated the effect of the argon metastable atoms on plasma properties in pure argon discharge. The plasma density in the case without metastable atoms was observed to be much higher than that with metastable atoms, especially at a higher voltage, a higher pressure, and/or a higher frequency. In 2010, Ohba *et al.*[11] measured the spatial distribution of argon metastable density in dual-frequency (DF) CCP by using a pair of optical emission lines. Also in DF-CCP, the tunable diode laser absorption spectroscopy (TDLAS) was used by Liu *et al.*[12] to investigate the dependence of argon metastable state density on rf power, pressure, and CF_4 content, and they found that the argon metastable state is mainly generated via the electron-impact excitation with the ground state and lost through diffusion and collision quenching processes with electrons and neutral molecules.

In addition, there are many investigations about argon metastable states in other types of plasma sources, such as inductively coupled plasmas,[13–16] surface-wave plasmas,[17,18] hollow cathode discharges,[19] and micro-discharge plasmas.[20,21] Generally speaking, almost all of the methods of measuring the metastable atom density are based on spectroscopy diagnostics, of which the AS is the most suitable way to obtain their absolute densities due to the non-radiative nature of the metastable state. However, AS was more used in other types of plasmas[13–15,17–21] than in CCP.[3,12]

Oxygen-containing plasma plays an important role in the ashing of the photoresist mask, removing polymer films, oxidation or deposition of thin film oxides and other processes.[1,2] Recently, many researches have focused on the Ar/O_2 mixture discharge because of their specific features both experimentally and theoretically.[7,22–28] For example, Takechi and Lieberman[23] found that argon addition into oxygen inductive discharges can greatly improve the plasma density and the etch rate due to the increased dissociation of O_2 by metastable argon atoms. In a capacitively coupled discharge, Worsley *et al.*[24] also observed that the O radical density is raised upon argon dilution as a result of an increasing contribution of Penning dissociation, which agreed well with the data simulated by Lee *et al.*[26] through using a PIC–MCC model. However, there are few researches about the density measurement of the argon metastable state in Ar/O_2 mixture capacitive discharges by using AS.

In this paper, densities of argon metastable states ($1s_5$ and $1s_3$) as a function of high-frequency (HF, 60 MHz) power, low-frequency (LF, 2 MHz) power, and working pressure in DF-CCP with three different gas components (0%, 5%, and 10% oxygen mixed in argon) are measured by the TDLAS. The effects of oxygen content on argon metastable state density are also studied at different pressures. Moreover, electron density is obtained by using a home-made hairpin probe to better understand the main generation and loss processes of the metastable states. The experimental details are briefly described in Section 2. Then in Section 3, experimental results are discussed. Finally, some conclusions are drawn from the present study in Section 4.

2. Experimental and data treatment details

The measurements were implemented in a 280 mm diameter cylindrical vacuum vessel as shown in Fig. 1. The vacuum vessel has been described in more detail elsewhere,[12,22,29] so only a brief description is given here. The plasma is produced between the two circular plate electrodes with 210 mm in diameter and 30 mm in spacing. The upper electrode is driven by the DF power sources (60/2 MHz, 1 kW, Thamway), while the bottom electrode and the vessel wall are grounded.

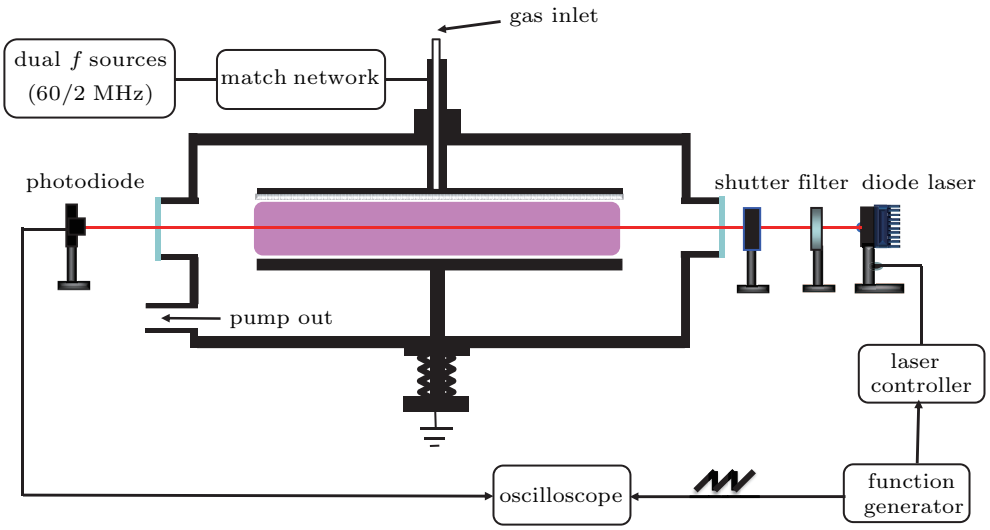


Fig. 1. (color online) Schematic of the DF capacitively coupled plasma reactor equipped with the tunable diode laser absorption spectroscopy (TDLAS) diagnostic system.

Argon metastable density is obtained by using the TD-LAS. A tunable diode laser (LD-0773-0075-DFB-1, Toptica) is used to launch a laser beam, which travels through the mid-gap between the two electrodes after being collimated via some apertures. After passing through the chamber, the laser beam is detected by a photodiode and displayed on a digital oscilloscope (LeCroy Waverunner). A neutral density filter is placed in front of the laser entrance of the chamber, aiming to avoid light saturation in the detection procedure by the photodiode. The shutter can manage the laser beam to enter into or be blocked out of the plasma chamber. It should be noted that the tunable diode laser is tuned by a current controller unit (LDC205, Thorlabs). The current can be controlled by a 10-Hz triangle voltage signal generated by a function generator in order to scan the profile of absorption peaks of argon metastable state over the wavelength range (772.3 nm–772.5 nm). The diode temperature is set to be at 31 °C by the temperature controller unit (TED 200 C, Thorlabs).

After the adjustment of the wavelength range, the following four spectral intensity profiles should be measured to determine the absolute concentration of the metastable atoms:[12,21,30,31]

(i) I_{P+L} when both laser and plasma are on;

(ii) I_P when plasma is on, and the laser beam is shut out by the shutter;

(iii) I_B when plasma is off and the laser beam is shut out by the shutter;

(iv) I_L when plasma is off, and the laser on.

Here, subscripts P, L, and B refer to plasma, laser, and background, respectively. At each of the discharge parameters, the four spectral intensity profiles I_{P+L}, I_P, I_B, and I_L need to be simultaneously measured within a short time to ensure the accuracy. Figure 2 shows a typical example of the four spectral lines obtained in the argon plasma driven at 60 MHz, 100 W, and 12 Pa.

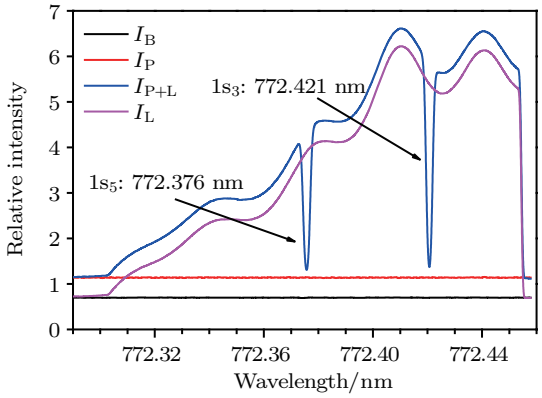


Fig. 2. (color online) Spectral profiles of I_{P+L}, I_P, I_B, and I_L in pure argon discharge driven at 60 MHz, 100 W, and 12 Pa.

Following steps described above, the laser intensity I_0 and its transmission beam intensity I_t can be written as follows: $I_0 = I_L - I_B$ and $I_t = I_{L+p} - I_p$.

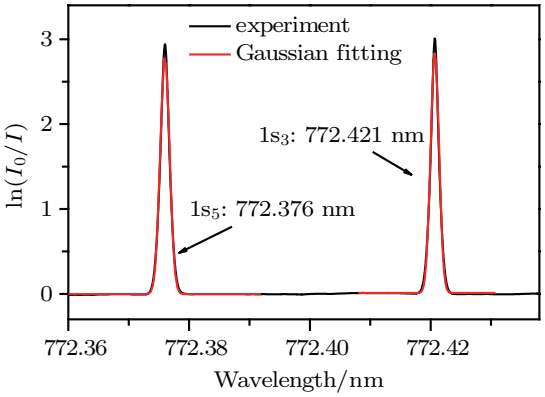


Fig. 3. (color online) Measured absorption rate profile (black dash curve) and Gaussian fitting curve (red solid curve) calculated from four spectral lines shown in Fig. 2: both peak at 772.376 nm and 772.421 nm.

Then, argon metastable density can be determined with the law of Beer–Lambert

$$I_t(v) = I_0(v)\, e^{-\sigma(v)Nl}, \tag{1}$$

where N is the absolute density of the metastable states, l is the absorption length (approximately equal to the chamber diameter in our experiment), and the absorption cross section $\sigma(v)$ can be expressed as

$$\sigma(v) = A_{21}\frac{\lambda^2 g_2}{8\pi g_1} f(v), \tag{2}$$

where $f(v)$ is the normalized Gaussian function, A_{21} is Einstein's coefficient, and g_1 and g_2 are the statistical weights of the lower and higher levels, respectively. Then, combining Eqs. (1) and (2), we can obtain the metastable density from

$$\begin{aligned} N &= \frac{8\pi g_1}{l\lambda^2 g_2 A_{21}} \int \ln\left(\frac{I_0(v)}{I_t(v)}\right) dv \\ &= \frac{8\pi g_1 c}{l\lambda^4 g_2 A_{21}} \int \ln\left(\frac{I_0(\lambda)}{I_t(\lambda)}\right) d\lambda. \end{aligned} \tag{3}$$

The integral in Eq. (3) is solved by a Matlab routine after a nonlinear Gaussian curve fitting.

In addition, a home-made hairpin probe is utilized to measure the electron density at the discharge center. In order to reduce the rf disturbance, the hairpin probe used in our experiment is fully floating and its detailed description can be found elsewhere.[22] The hairpin probe is based on the microwave resonance theory, which was developed by Piejak *et al.*[32,33] and Curley.[34] The electron density can be obtained from the following expression

$$n_e = \frac{f_p^2 - f_0^2}{0.81}\left(10^{10}\ \mathrm{cm}^{-3}\right), \tag{4}$$

where n_e is the electron density, f_p and f_0 (with unit of GHz) are the resonant frequencies of the hairpin probe in plasma and vacuum, respectively.

3. Results and discussion

In this section, the effects of HF and LF powers, working pressure, and oxygen content on densities of argon metastable states ($1s_5$ and $1s_3$) are studied. The main production and loss processes of metastable states are analyzed in Subsection 3.1. In Subsections 3.2–3.5, experimental results and a discussion are presented.

3.1. Main production and loss processes of metastable states

As the argon $1s_3$ state exhibits similar production and loss processes to the $1s_5$ state, thus only the $1s_5$ was analyzed here. The $1s_5$ density is governed by the following one-dimensional continuity equation[3]

$$\frac{\partial n_{\rm m}}{\partial t} = F_{\rm m}(t) - L_{\rm m}(t) - G_{\rm m}(t), \tag{5}$$

where $n_{\rm m}$ is the metastable density, $F_{\rm m}(t)$ is the production rate, $L_{\rm m}(t)$ is the loss rate due to the collision process with other species, and $G_{\rm m}(t)$ is the diffusion loss rate, denoted by the subscript m. For a steady plasma, equation (5) can be written as

$$F_{\rm m} = L_{\rm m} + G_{\rm m}. \tag{6}$$

The production of argon metastable atoms is principally from the process of direct electron-impact excitation with the argon ground state: $\mathrm{Ar}(g) + \mathrm{e} \rightarrow \mathrm{Ar_m} + \mathrm{e}$. Other processes such as ion-impact excitation and radiative transition from higher excited states can be ignored due to lower densities than that at the argon ground state, and smaller reaction coefficients.[3,4,12] Thus, $F_{\rm m}$ can be given by

$$F_{\rm m} = n_{\rm Ar(g)} n_{\rm e} k_{\rm ge}, \tag{7}$$

where $n_{\rm Ar(g)}$ is the density of argon atoms at ground state, $n_{\rm e}$ is the electron density, and $k_{\rm ge}$ is the rate coefficient of electron impact excitation from the argon ground state to the metastable state.

In pure argon discharges, the primary loss processes of the argon metastable state are from electron impact, i.e., the metastable argon atoms might be excited to 2p-levels, resonant and ionized states via these reactions like (i) $\mathrm{Ar_m} + \mathrm{e} \rightarrow \mathrm{Ar}(2\mathrm{p_n}) + \mathrm{e}$, (ii) $\mathrm{Ar_m} + \mathrm{e} \rightarrow \mathrm{Ar_r} + \mathrm{e}$, (iii) $\mathrm{Ar_m} + \mathrm{e} \rightarrow \mathrm{Ar^+} + \mathrm{e}$. Other impact loss processes by electrons and ground argon atoms could be ignored due to lower rate coefficients.[3,4] While in the argon–oxygen mixed gas discharge, the main loss channel could be the quenching collision process by O_2 molecules: (iv) $\mathrm{Ar_m} + \mathrm{O_2} \rightarrow \mathrm{O_2} + \mathrm{Ar}$. So, we can give the following expression of the loss rate by these collision processes:

$$\begin{aligned} L_{\rm m} &= (k_{\rm exc} + k_{\rm res} + k_{\rm ion}) n_{\rm e} n_{\rm m} + k_{q\rm O_2} n_{\rm O_2} n_{\rm m} \\ &= k_{\rm qe} n_{\rm e} n_{\rm m} + k_{q\rm O_2} n_{\rm O_2} n_{\rm m}, \end{aligned} \tag{8}$$

where $k_{\rm qe} = k_{\rm exc} + k_{\rm res} + k_{\rm ion}$ is the total collision quenching rate of the metastable state by electrons as listed in reactions (i)–(iii), and $k_{q\rm O_2}$ is the collision quenching rate by O_2 molecules, $n_{\rm m}$ is the metastable density, and $n_{\rm O_2}$ is the oxygen molecule density. As for the axial diffusion loss, the loss rate can be written as

$$G_{\rm m} \approx \frac{D_{\rm m}}{\Lambda^2 p} n_{\rm m} = k_{\rm D} n_{\rm m}, \tag{9}$$

where $D_{\rm m}$ is the metastable diffusion coefficient, $\Lambda \approx L/\pi$ is the characteristic length with L being the inter-electrode distance, p is the working pressure, and $k_{\rm D}$ is the effective diffusive loss rate of the metastable state. Therefore, a new equation that is derived from Eqs. (5)–(9) can be obtained as follows:

$$n_{\rm m} = \frac{n_{\rm Ar(g)} n_{\rm e} k_{\rm ge}}{k_{\rm D} + k_{\rm qe} n_{\rm e} + k_{q\rm O_2} n_{\rm O_2}}. \tag{10}$$

In this equation, the rate coefficients of the main production and loss process for metastable atoms are listed in Table 1, where E_j is the energy threshold in each reaction.

Table 1. Rate coefficients of the main production and loss processes for the metastable atoms.[1,25,35,36]

Reactions	Rate coefficients/$\mathrm{cm^3 \cdot s^{-1}}$	E_j/eV	References
$\mathrm{Ar(g)} + \mathrm{e} \rightarrow \mathrm{Ar_m} + \mathrm{e}$	$k_{\rm ge} = 3.71 \times 10^{-8} \times \mathrm{e}^{-15.06/T_{\rm e}}$	11.56[a]	[35]
$\mathrm{Ar_m} + \mathrm{e} \rightarrow \mathrm{Ar^+} + 2\mathrm{e}$	$k_{\rm ion} = 2.05 \times 10^{-7} \times \mathrm{e}^{-4.95/T_{\rm e}}$	4.14[a]	[25]
$\mathrm{Ar_m} + \mathrm{e} \rightarrow \mathrm{Ar_r} + \mathrm{e}$	$k_{\rm res} = 2 \times 10^{-7}$	0.1[b]	[1]
$\mathrm{Ar_m} + \mathrm{e} \rightarrow \mathrm{Ar}(2\mathrm{p_n}) + \mathrm{e}$	$k_{\rm exc} = 1.26 \times 10^{-6} \times \mathrm{e}^{-2/T_{\rm e}}$	/	[36]
$\mathrm{Ar_m} + \mathrm{O_2} \rightarrow \mathrm{Ar} + \mathrm{O_2}$	$k_{q\rm O_2} = 1.12 \times 10^{-9}$	/	[25]

[a]Two metastable levels $3P_0$ and $3P_2$ in the $3p^5 4s$ configuration are combined into one composite level.
[b]Reaction energy threshold is very low and the value is about 0.1 eV.

It can be clearly seen that the electron density $n_{\rm e}$ and oxygen molecule density $n_{\rm O_2}$ have great influences on the metastable state density. The electron temperature $T_{\rm e}$ also has an effect on the density of metastable atoms by affecting rate coefficients. More discussion will be presented based on our experimental results in the following subsections.

3.2. HF power effect

In this subsection, densities of argon $1s_5$ and $1s_3$ states and electron as a function of HF power $P_{\rm H}$ in single-frequency

(SF) and DF capacitive discharges with different gas components (0%, 5%, and 10% oxygen mixed in argon) are investigated. Note that the working pressure is fixed at 13 Pa, and in the DF discharge, LF power P_L is fixed at 50 W. The experimental results in SF and DF cases are presented in Figs. 4 and 5, respectively. One can see from Figs. 4 and 5 that the two metastable state densities exhibit similar dependence on P_H. To simplify the analysis, more attention is paid to the analysis of the $1s_5$ state.

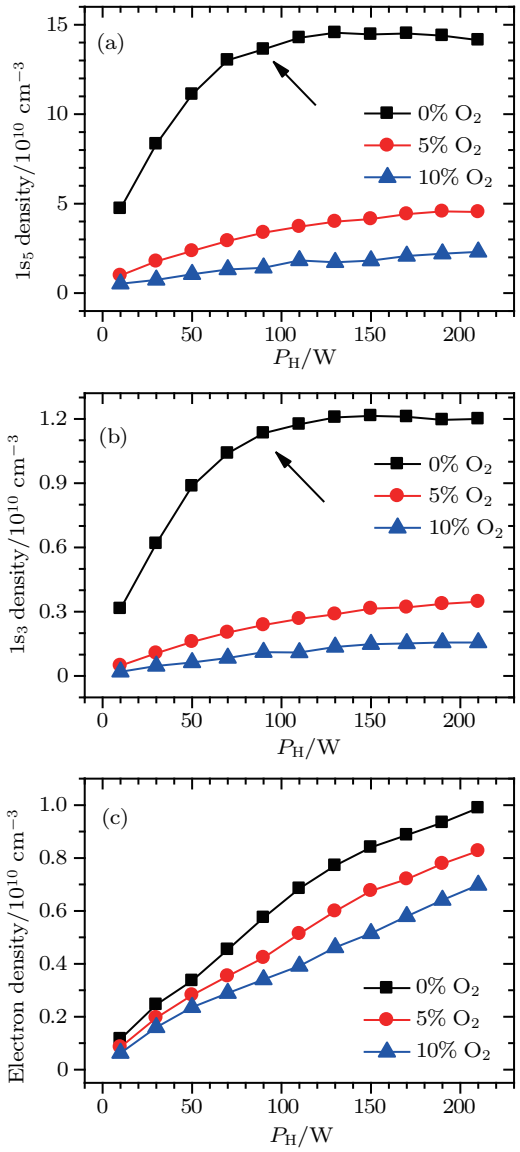


Fig. 4. (color online) Variations of (a) $1s_5$, (b) $1s_3$, and (c) electron densities with HF power P_H in SF driven discharge with different gas components (0%, 5%, and 10% oxygen mixed in argon). Pressure is fixed at 13 Pa. Note that arrows in panels (a) and (b) roughly indicate the saturation points of the metastable densities.

In the SF case, taking $1s_5$ for example (see Fig. 4(a)), with the increase of P_H, the metastable density in the pure argon discharge (the black curve with squares) first rises rapidly and then becomes saturated at a value about 1.4×10^{11} cm^{-3} at $P_H > 90$ W. By contrast, electron density increases almost linearly with P_H increasing as shown in Fig. 4(c). The different loss processes can explain the different dependence of $1s_5$ and electron densities on P_H, because electron and $1s_5$ state have similar generation processes.

The increasing electron density with P_H increasing is attributed to the enhancement of the electron-impact ionization reaction with argon ground-state atoms. Similarly, the generation of the $1s_5$ state is dominated by the collision excitation process of high-energy electrons (above 10 eV) with ground-state argon atoms. However, besides the diffusion loss process when compared with electrons, the additional quenching loss process of $1s_5$ by collisions with lower-energy electrons (only several eV or even lower) plays an important role. As P_H increases, the quenching loss of the $1s_5$ state by electron collision is enhanced due to the rising of the electron and $1s_5$ state density. As a result, the $1s_5$ density tends to be saturated at a higher value of P_H.

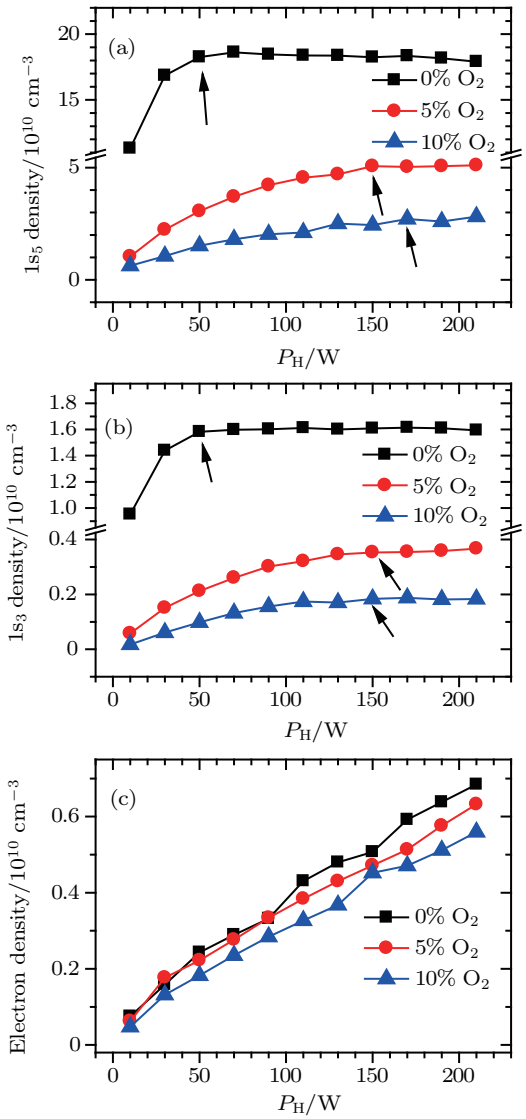


Fig. 5. (color online) Variations of (a) $1s_5$, (b) $1s_3$, and (c) electron densities with P_H in DF driven discharge with different gas components (0%, 5%, 10% oxygen mixed in argon). LF power P_L and working pressure are fixed at 50 W and 13 Pa, respectively. Note that arrows in panels (a) and (b) roughly indicate the saturation points of the metastable state densities.

Figure 4(b) illustrates the evolution of $1s_3$ state density with P_H. We can see that the variation of $1s_3$ state density with P_H shows the same manners as that of $1s_5$ state density because they are at similar energy levels. It should be noted that the $1s_3$ state density is about one order of magnitude lower than the $1s_5$ state due to their larger difference in degeneracy.[12,37] Besides, it can be seen from Figs. 4(a) and 4(b) that the $1s_5$ or $1s_3$ state densities in the Ar/O_2 mixture discharges (5% and 10% oxygen in argon) rise more slowly with increasing P_H than that in the pure argon. This is because in Ar/O_2 mixture discharges the metastable-state density is largely depleted due to the quenching loss process by oxygen molecules. At $P_H = 90$ W, for instance, an addition of 5% oxygen can reduce the $1s_5$ state density by 75%, i.e., from 13.63×10^{10} cm^{-3} to 3.38×10^{10} cm^{-3}. Therefore, the metastable density in gas mixture discharges does not come to the saturation at higher P_Hs under the present experimental condition. The quenching loss rate of the metastable state via collisions with oxygen molecules remains almost unchanged with increasing P_H when oxygen content and working pressure are fixed. So we can expect that the density of metastable atoms in discharges of gas mixture will also come to a saturation value at a much higher value of P_H

The dependence of $1s_5$, $1s_3$, and electron densities on P_H is also investigated in DF CCP, and the results under otherwise identical conditions as in Fig. 4 are shown in Fig. 5. It can be seen that the metastable state densities change with increasing P_H in a similar fashion to that in the SF case (in Fig. 4). Also taking the $1s_5$ state in pure argon for example (the black curve with squares in Fig. 5(a)), we can see that as P_H increases, its density in the DF case first rises rapidly and then reaches a saturation value at $P_H = 50$ W, which is smaller than that (90 W) in the SF case. Moreover, for the DF discharge operated in gas mixtures (5% and 10% oxygen in argon), it is observed that the metastable state density with increasing P_H reaches a saturation value at $P_H > 110$ W. The metastable state density in the DF case is higher than that in the SF case, although the electron density behavior is different. These will be discussed in detail in Subsection 3.3.

3.3. LF power effect

In Subsection 3.2, it has been seen that the variation of metastable state density in the DF case with P_H is somewhat different from that in the SF case. In order to analyze their difference, we compare the dependence of the metastable state and electron densities on P_H in the pure argon discharge driven by SF source with that by DF sources in Fig. 6. Note that the data shown in Figs. 6(a)–6(c) are exactly the same as in Figs. 4 and 5. The electron temperature shown in Fig. 6(d) is measured by a floating double probe. It can be observed from Figs. 6(a) and 6(b) that the metastable state densities in the DF case rise much faster with P_H increasing and come to their corresponding saturation values at a lower P_H than in the SF case. The density values of metastable states in the DF case are higher than in the SF case at the same P_H. This is mainly because higher electron temperature in the DF case (about 2 eV higher than in the SF case, see Fig. 6(d)) will lead the rate constant k_{ge} to increase and, consequently, the more metastable atoms to

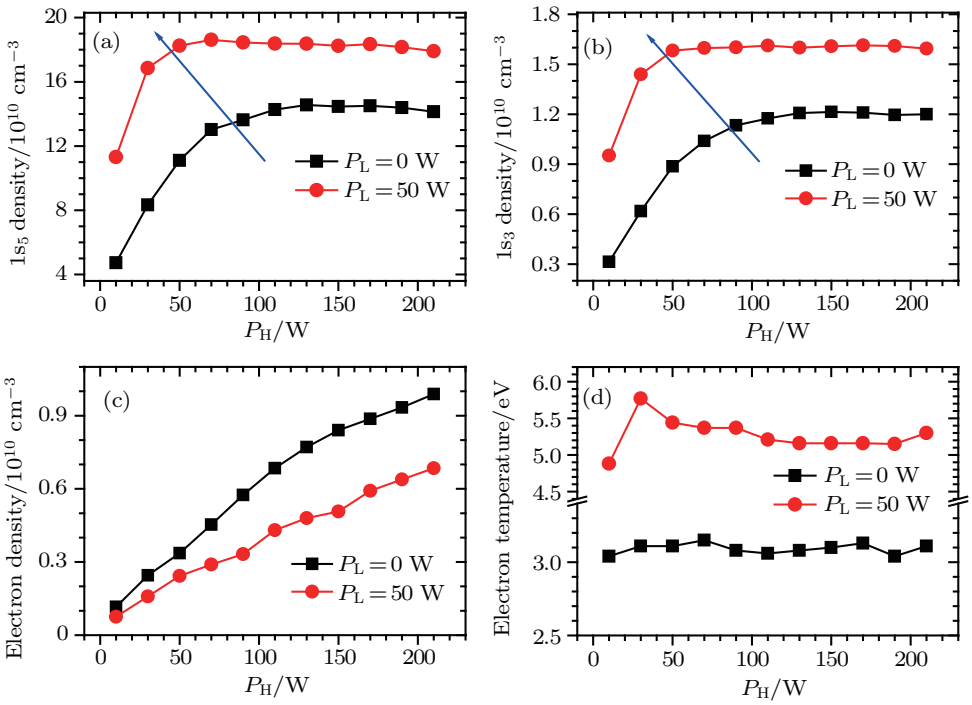


Fig. 6. (color online) Comparison among variations of (a) $1s_5$ and (b) $1s_3$, (c) electron densities, and (d) electron temperature with P_H in SF and DF discharges operated in pure argon. Note the data in panels (a)–(c) are exactly the same as those in Figs. 4 and 5.

be produced via electron-impact excitation with ground-state atoms. However, it can be seen from Fig. 6(c) that the electron density in the SF case is higher than that in the DF case (see Fig. 6(c)). This could be due to the fact that in the DF case the fraction of high energy electrons (with energy higher than the excitation threshold of metastable states) is much higher than in the SF discharge because of enhanced electron heating by the LF source, so that the production of metastable atoms could still be improved.

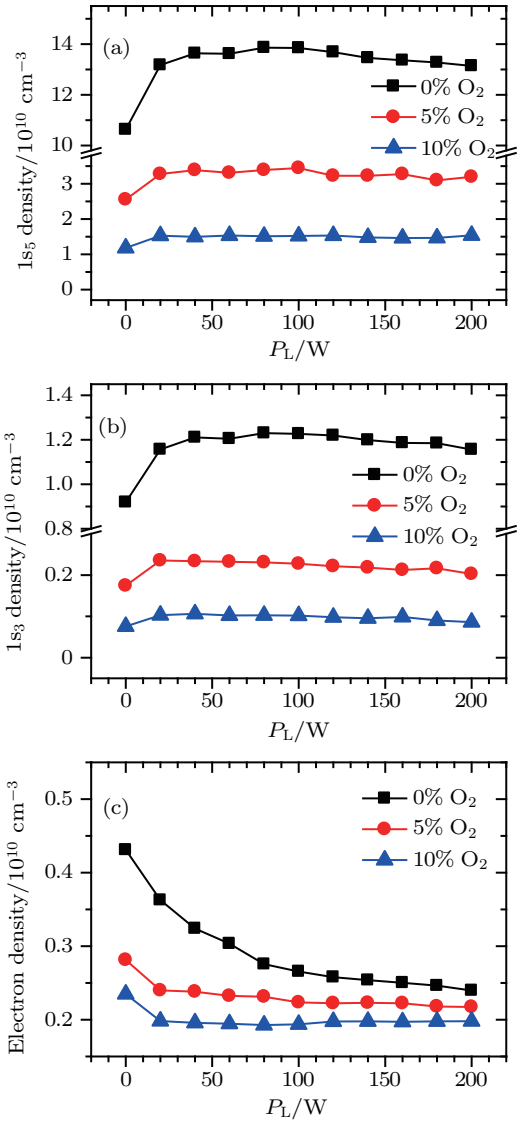


Fig. 7. (color online) Variations of (a) $1s_5$, (b) $1s_3$, and (c) electron densities with LF power P_L in DF discharges with different gas components (0%, 5%, and 10% oxygen mixed in argon). Value of P_H is fixed at 50 W and working pressure is fixed at 13 Pa.

Figure 7 displays the variations of $1s_5$, $1s_3$, and electron densities with P_L increasing in the DF driven discharges with different gas components (0%, 5%, and 10% oxygen in argon). HF power and working pressure are fixed at 50 W and 13 Pa, respectively. It can be clearly seen from Figs. 7(a) and 7(b) that the densities of $1s_5$ and $1s_3$ states each exhibit an evident increase when the LF power of 20 W is applied. However, the metastable densities are almost independent of P_L at higher values of P_L. This can be explained by a combined effect of increased electron temperature and shrinking plasma bulk length. In the case of the LF power, on the one hand, the electron temperature increases obviously, and thus raises the production rate of the metastable state atoms, which is similar to the results in Fig. 6. On the other hand, the higher P_L enlarges the plasma sheath width, and thus the plasma bulk volume shrinks, leading to the decrease of the volume, in which metastable states can be effectively produced via electron impact. Because of the balance between the two factors, the metastable state density remains unchanged as the value of P_L varies.

3.4. Pressure effect

Figure 8 exhibits the dependence of $1s_5$ and $1s_3$ states and electron densities on working pressure (from 2 Pa to 28 Pa) in the DF driven discharges with different gas components (0%, 5%, and 10% oxygen mixed in argon). The values of P_H and P_L are fixed at 100 W and 50 W, respectively. In the pure argon discharge, one can see from the curve with black squares in Fig. 8(a) that $1s_5$ state density increases rapidly when the pressure is raised from 2 Pa to 16 Pa, and then it decreases slightly with the further increase of pressure. By contrast, when the argon discharge is diluted with 5% oxygen (the curve with red circles in Fig 8(a)), the $1s_5$ state density increases with pressure at the low-pressure end and then decreases almost linearly after its maximum at $p = 6$ Pa. When the oxygen content increases to 10%, the $1s_5$ state density actually shows a linear decrease with pressure, indicating that the maximum density shifts to a lower pressure. Compared with the variation of the $1s_5$ density with pressure, the variation of electron density shows almost the same dependence on pressure in discharges with different oxygen content. Taking the pure argon discharge for example, the electron density increases rapidly in a pressure range of 2 Pa–6 Pa and then decreases with pressure further increasing.

The dependence of the metastable density on pressure could be understood as follows. In the pure argon discharge operated at lower pressure, the groundstate atom density rising with pressure results in the enhancement of the production rate of the argon metastable state due to the increasing electronic excitation rate. Therefore, the metastable density increases rapidly at $p < 16$ Pa. However, at higher pressures, the electron-neutral collision is intensified, leading to the decrease of the electron temperature and, consequently, the decrease of the electron density. This is the reason why the $1s_5$ state density comes to a saturation value and even shows a slight decay at higher pressures.

At 5% oxygen content, the variation of $1s_5$ state density with pressure behaves similarly to that of the electron density. When argon plasma is diluted by 10% oxygen, it seems that

argon $1s_5$ state density reaches a maximum value at $p = 2$ Pa or 4 Pa, and decreases linearly with pressure increasing, as shown in Fig 7(a). In a pure argon discharge, the changes of $1s_5$ and $1s_3$ with the pressure behave quite similarly, while in argon discharge with 5% or 10% oxygen dilution, it seems that the $1s_3$ density exhibits weaker dependence on pressure than $1s_5$ density. As the working pressure increases, $1s_3$ density shows a slight increase at $p < 10$ Pa, and then a slow decline at higher pressures, which is true for both 5% and 10% oxygen dilution cases.

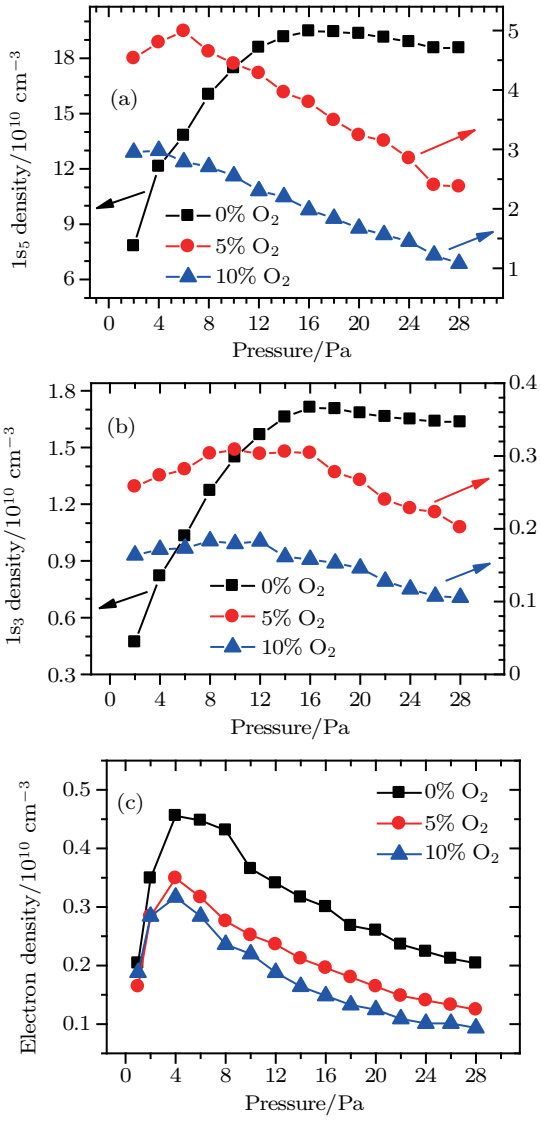


Fig. 8. (color online) Variations of (a) $1s_5$, (b) $1s_3$, and (c) electron densities with working pressure in the DF discharges with different gas components (0%, 5%, and 10% oxygen mixed in argon). Values of P_H and P_L are fixed at 100 W and 50 W, respectively.

3.5. Oxygen content effect

Figure 9 shows $1s_5$, $1s_3$, and electron densities as a function of oxygen content at three different working pressures (6.7 Pa, 13 Pa, and 20 Pa). The values of P_H and P_L are fixed at 100 W and 50 W, respectively. From Figs. 9(a) and 9(b), one can clearly see that adding a small fraction of oxygen will significantly reduce the densities of $1s_5$ and $1s_3$ states. Taking $1s_5$ at 20 Pa for example (the curve with blue triangles in Fig. 9(a)), with an addition of 5% oxygen, its density is reduced by 77%, i.e., from 18.50×10^{10} cm^{-3} to 4.15×10^{10} cm^{-3}. By contrast, the electron density (see Fig. 9 (c)) falls by 19% at 20 Pa when adding 5% oxygen in argon. The dramatic depletion of metastable states can be understood with Eq. (10) in Subsection 3.1. The electron temperature remains almost the same by adding 5% oxygen in argon,[38] and the discharge structure or electric field structure is weakly influenced by the oxygen dilution, so that the electron power absorption mode remains unchanged. Therefore, the production rate of the metastable state is believed to change slightly when only 5% oxygen is added. The sharp fall of the metastable density is mainly attributed to the quenching loss process by oxygen molecules, because the diffusion loss rate k_D and quenching loss rate

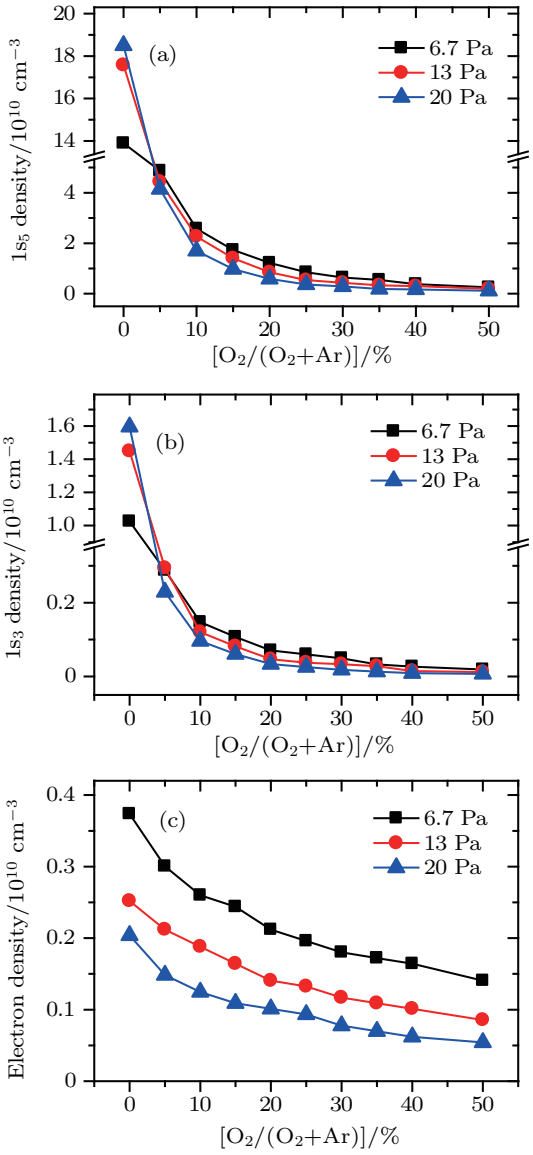


Fig. 9. (color online) Variations of (a) $1s_5$, (b) $1s_3$, and (c) electron densities with oxygen content in DF driven discharges at three different gas pressures (6.7 Pa, 13 Pa, and 20 Pa). Values of P_H and P_L are fixed at 100 W and 50 W, respectively.

by electrons, $k_{qe}n_e$, show much weaker dependence on the oxygen fraction than the quenching loss rate by the oxygen molecule, which has a relatively high rate coefficient k_{qO_2}.

With the increase of pressure, it can be seen from Figs. 9(a) and 9(b) that Ar $1s_5$ and $1s_3$ densities show more remarkable decreases with oxygen content, indicating that the quenching loss by oxygen molecules is enhanced at a higher pressure. To be more specific, at 6.7 Pa and 13 Pa, with 5% oxygen dilution, the values of $1s_5$ density decrease by 65% and 75%, respectively. When pressure increases to 20 Pa, the $1s_5$ density decreases by 77%. This phenomenon is consistent with that in Subsection 3.4.

4. Conclusions

In this paper, we have measured the densities of two metastable states ($1s_5$ and $1s_3$) in argon and argon/oxygen mixture DF-CCP by using the tunable diode laser absorption spectroscopy. Effects of HF power, LF power, and working pressure on the metastable state density are studied in discharges operated with different gas components (0%, 5%, and 10% oxygen mixed in argon). The dependence of the metastable state density on oxygen content is also investigated at different working pressures. It is found that the metastable state densities exhibit different dependence on HF power in discharges with different content of oxygen added in argon. As HF power increases, the metastable density in the pure argon discharge first increases rapidly and then tends to be saturated at higher HF powers. When the argon plasma is diluted with 5% or 10% oxygen, metastable state density would be saturated at a higher HF power than the case of pure argon plasma. In DF-CCP, LF power is found to weakly affect the metastable state density. With the increase of working pressure, the metastable state density first increases, and then decreases slowly after reaching its peak value. The pressure value at which the maximum metastable density occurs decreases with the increase of the oxygen content. A small fraction of oxygen will greatly deplete the metastable state atoms, and this becomes more significant at a higher pressure due to the enhanced quenching process by oxygen molecules.

References

[1] Lieberman M A and Lichtenberg A J 2005 *Principles of Plasma Discharges and Materials Processing*, 2nd edn. (New York: Wiley-Interscience)

[2] Chabert P and Braithwaite N 2011 *Physics of radio-frequency plasmas* (Cambridge: Cambridge University Press)

[3] Sansonnens L, Howling A A, Hollenstein C, Dorier J-L and Kroll U 1994 *J. Phys. D: Appl. Phys.* **27** 1406

[4] Zhang Y R, Xu X and Wang Y N 2010 *Phys. Plasmas* **17** 033507

[5] Katori H and Shimizu F 1993 *Phys. Rev. Lett.* **70** 3545

[6] Mityureva A A and Smirnov V V 2004 *Opt. Spectrosc.* **97** 508

[7] Kitajima T, Nakano T and Makabe T 2006 *Appl. Phys. Lett.* **88** 091501

[8] Mcmillin B K and Zachariah M R 1995 *J. Appl. Phys.* **77** 5538

[9] Mcmillin B K and Zachariah M R 1996 *J. Appl. Phys.* **79** 77

[10] Rauf S and Kushner M J 1997 *J. Appl. Phys* **82** 2805

[11] Ohba T and Makabe T 2010 *Appl. Phys. Lett.* **96** 111501

[12] Liu W Y, Xu Y, Liu Y X, Peng F, Guo Q, Li X S, Zhu A M and Wang Y N 2015 *J. Appl. Phys.* **117** 023306

[13] Hayashi Y, Hirao S, Zhang Y, Gans T, O'Connell D, Petrović Z L and Makabe T 2009 *J. Phys. D: Appl. Phys.* **42** 145206

[14] Bakowski B, Hancock G, Peverall R, Prince S E, Ritchie G A D and Thornton L J 2005 *J. Phys. D: Appl. Phys.* **38** 2769

[15] Bol'shakov A A and Cruden B A 2008 *Tech. Phys.* **53** 1423

[16] Sato T and Makabe T 2005 *J. Appl. Phys* **98** 113304

[17] Muñoz J, Margot J and Calzada M D 2012 *J. Appl. Phys.* **111** 023303

[18] Hübner S, Sadeghi N, Carbone E A D and van der Mullen J J A M 2013 *J. Appl. Phys.* **113** 143306

[19] Bánó G and DonkóZ 2012 *Plasma Sources Sci. Technol.* **21** 035011

[20] Belostotskiy S G, Ouk T, Donnelly V M, Economou D J and Sadeghi N 2011 *J. Phys. D: Appl. Phys.* **44** 145202

[21] Cooley J, Xue J and Urdahl R 2012 *J. Phys. D: Appl. Phys.* **45** 365201

[22] Liu J, Wen D Q, Liu Y X, Gao F, Lu W Q and Wang Y N 2013 *J. Vac. Sci. Technol. A* **31** 061308

[23] Takechi K and Lieberman M A 2001 *J. Appl. Phys.* **90** 3205

[24] Worsley M A, Bent S F, Fuller N C M and Dalton T 2006 *J. Appl. Phys.* **74** 083301

[25] Lee C and Lieberman M A 1995 *J. Vac. Sci. Technol. A* **13** 368

[26] Lee S H, Iza F and Lee J K 2006 *Phys. Plasmas* **13** 057102

[27] Liu J, Zhang Q Z, Liu Y X, Gao F and Wang Y N 2013 *J. Phys. D: Appl. Phys.* **46** 235202

[28] Wang Y H, Liu W, Zhang Y R and Wang Y N 2015 *Chin. Phys. B* **24** 095203

[29] Liu Y X, Liang Y S, Wen D Q, Bi Z H and Wang Y N 2015 *Plasma Sources Sci. Technol.* **24** 025013

[30] Dittmann K 2009 "Detailed Investigations of the Sheath Dynamics and Elementary Processes in Capacitively Coupled RF Plasmas", Ph. D. dissertation (Greifswald: University of Greifswald)

[31] Jiang X Z, Liu Y X, Bi Z H, Lu W Q and Wang Y N 2012 *Acta Phys. Sin.* **61** 015204 (in Chinese)

[32] Piejak R B, Godyak V A, Garner R, Alexandrovich B M and Sternberg N 2004 *J. Appl. Phys.* **95** 3785

[33] Piejak R B, Alkuzee J and Braithwaite N S J 2005 *Plasma Sources Sci. Technol.* **14** 734

[34] Curley G A, Marić D, Booth J P, Corr C S, Chabert P and Guillon J 2007 *Plasma Sources Sci. Technol.* **16** S87

[35] Bukowski J D, Graves D B and Vitello P 1996 *J. Appl. Phys.* **80** 2614

[36] Zhu X M and Pu Y K 2010 *J. Phys. D: Appl. Phys.* **43** 403001

[37] Ferreira C M, Loureiro J and Ricard A 1985 *J. Appl. Phys.* **57** 82

[38] Monahan D D and Turner M M 2008 *Plasma Sources Sci. Technol.* **17** 045003